ISSN 1749-3889 (print), 1749-3897 (online)
International Journal of Nonlinear Science
Vol.27(2019) No.2,pp.107-122

Stability of The Collinear Points with Perturbing Forces in The Relativistic R3BP

Nakone Bello[1] *, Aminu Abubakar Hussain[2]
[1] Department of Mathematics, Faculty of Science, Usmanu Danfodiyo University, Sokoto, Nigeria
[2] Department of Mathematics, Faculty of Natural and Applied Sciences, Nasarawa State University, Keffi, Nigeria
(Received 20 May 2018, accepted 17 October 2018)

Abstract: In this paper, locations and stability of the collinear points are investigated within the framework of the Post-Newtonian approximation when the more massive primary is an oblate spheroid. A numerical exploration in this connection with Jupiter-Satellite systems and Saturn-Satellite systems reveals that the points L_1 and L_2 moves towards the smaller primary due to oblateness and relativistic factors while L_3 moves away from the bigger primary due to oblateness. Also the locations of these points are drawn versus the mass ratio μ and it is observed that the point L_1 moves away from the smaller primary for an increasing mass ratio while L_2 moves towards the bigger primary when the mass ratio increases. The point L_3 moves away from the bigger primary when the mass ratio increases. It is also noticed that only point L_2 is significantly affected by the relativistic effect when varying the mass ratio. The collinear points are found to be unstable due to the presence of positive real roots.

Keywords: Collinear points; Post-Newtonian approximation; Oblate spheroid; Oblateness

1 Introduction

The restricted three-body problem with oblateness of the primaries has received attention with respect to its five equilibrium points, i.e. the collinear point L_1, L_2, and L_3 and the triangular points L_4 and L_5, see (SubbaRao and Sharma [1], Sharma and SubbaRao [2], Sharma [3], Abouelmagd [4]). Anderson et al. [5] computed the families of orbits focusing on orbits with multiple loop near the secondary in the Jupiter-Europa system and explored also their characteristics. Ershkov [6] studied the Yarkovsky effect in generalized photogravitational 3-body problem. The relativistic effect also plays a key role in the restricted three-body problem. The relativistic restricted three-body was originally studied by Brumberg [7].

Bhatnagar and Hallan [8] studied the linear stability of the relativistic triangular points L_4 and L_5 and it was shown that these points are stable for the whole range $0 \leq \mu \leq \frac{1}{2}$, despite it is known that the non-relativistic points L_4 and L_5 are stable for $\mu < \mu_0$, where $\mu_0 = 0.038521$ (Szebehely [9]) is the Routh critical mass ratio. The same model problem was later investigated by Douskos and Perdios [10] and Ahmed et al. [11], who found respectively the range of stability of triangular points as $0 \leq \mu < \mu_0 - \frac{17\sqrt{69}}{486c^2}$ and $0 \leq \mu < 0.03840$, where c is the dimensional speed of light.

Recently, Singh and Bello [12, 13] have also studied the locations and stability of the same model problem under various different sources of perturbations such as centrifugal force and radiation. They found that in the absence of perturbations, their results are in agreement with those of Douskos and Perdios [10] and in disagreement with those of Bhatnagar and Hallan [8] and with those of Ahmed et al. [11].

Although there are many studies on the stability of triangular points in the relativistic R3BP, there are only few studies regarding stability of collinear points. The collinear points L_1 and L_2 are most interesting for space mission design due to their fast instability. This instability has already been used in consuming small expenditure of fuel presumably needed to keep a spacecraft there. Ragos et al. [14] studied the existence, position and stability of collinear points of the relativistic R3BP and they obtained the numerical results for all Sun-Planet pairs of our solar system. In recent years, (Abd El-Bar and Abd El-Salam [15], Abd El-Bar and Abd El-Salam [16], Abd El-Salam and Abd El-Bar [17], Katour et al. [18]) have carried out a number of studies on the locations of collinear points without studying their linear stability under various

*Corresponding author. *E-mail address*: bnakone@yahoo.com (N. Bello), dadinduniya@gmail.com (A.A. Hussain)

IJNS.2019.04.15/1037

aspect of perturbations such as radiation and oblateness. Pushparad and Sharma [19] studied the oblateness effect of Saturn on halo orbits of $L_1 \; and \, L_2$ in Saturn-Satellites restricted three-body problem. They found that L_1 and L_2 move towards Saturn with oblateness. Abd El-Bar et al. [20] computed the perturbed location of L_1 in the photogravitational with oblate primaries relativistic restricted three-body problem and obtained a series form of the location of this point as a new analytical result. They have also drawn the location of L_1 versus the mass ratio μ taking into account one or more of the considered perturbations. Abd El-Salam et al. [21] studied the location of equilibrium point L_1 in the photogravitational oblate relativistic R3BP with application on Sun-planet. Bello and Hussain [22] examined the stability of collinear points in the relativistic R3BP when the bigger primary is a triaxial rigid body. It raised a curiosity in our minds to study the effect of oblateness of the bigger primary on the stability of collinear points in the relativistic restricted three-body problem.

This paper is organized as follows. In Sect. 2, the equations governing the motion are presented; Sect. 3 describes the positions of collinear points, while their linear stability is analyzed in Sect. 4. A numerical application of these results and discussion are given in Sect. 5, and Sect. 6, respectively. Finally, Sect. 7 conveys the main findings of this paper.

2 The equations of motion

The pertinent equations of motion of an infinitesimal mass in the relativistic R3BP when the bigger primary is an oblate spheroid, in a barycentric synodic coordinate system (ξ, η) and dimensionless variables, can be written as Brumberg [7] and Bhatnagar and Hallan [8]:

$$\begin{aligned} \ddot{\xi} - 2n\dot{\eta} &= \tfrac{\partial W}{\partial \xi} - \tfrac{d}{dt}\left(\tfrac{\partial W}{\partial \dot{\xi}}\right), \\ \ddot{\eta} + 2n\dot{\xi} &= \tfrac{\partial W}{\partial \eta} - \tfrac{d}{dt}\left(\tfrac{\partial W}{\partial \dot{\eta}}\right), \end{aligned} \tag{1}$$

with

$$\begin{aligned} W = {} & \tfrac{1}{2}n^2\left(\xi^2+\eta^2\right) + \tfrac{1-\mu}{\rho_1}\left(1+\tfrac{A_1}{2\rho_1^2}\right) + \tfrac{\mu}{\rho_2} + \tfrac{1}{c^2}\left[\tfrac{1}{8}\left\{\dot{\xi}^2+\dot{\eta}^2+2n(\xi\dot{\eta}-\eta\dot{\xi})+n^2(\xi^2+\eta^2)\right\}^2\right. \\ & +\tfrac{3}{2}\left(\tfrac{1-\mu}{\rho_1}\left(1+\tfrac{A_1}{2\rho_1^2}\right)+\tfrac{\mu}{\rho_2}\right)\left\{\dot{\xi}^2+\dot{\eta}^2+2(\xi\dot{\eta}-\eta\dot{\xi})+(\xi^2+\eta^2)\right\} - \tfrac{1}{2}\left(\tfrac{(1-\mu)^2}{\rho_1^2}\left(1+\tfrac{A_1}{2\rho_1^2}\right)^2+\tfrac{\mu^2}{\rho_2^2}\right) \\ & +\mu(1-\mu)\left\{n\left(4\dot{\eta}+\tfrac{7}{2}n\xi\right)\left(\tfrac{1}{\rho_1}\left(1+\tfrac{A_1}{2\rho_1^2}\right)-\tfrac{1}{\rho_2}\right) - \tfrac{n^2\eta^2}{2}\left(\tfrac{\mu}{\rho_1^3}\left(1+\tfrac{A_1}{2{\rho_1}^2}\right)+\tfrac{1-\mu}{\rho_2^3}\right)\right. \\ & \left.\left. +n^2\left(-\tfrac{1}{\rho_1\rho_2}\left(1+\tfrac{A_1}{2{\rho_1}^2}\right)+\tfrac{\mu}{2\rho_1}\left(1+\tfrac{A_1}{2{\rho_1}^2}\right)-\tfrac{(1-\mu)}{2\rho_1}\left(1+\tfrac{A_1}{2\rho_1^2}\right)+\tfrac{1-3\mu}{2\rho_2}\right)\right\}\right], \end{aligned} \tag{2}$$

$$\begin{aligned} \rho_1^2 &= (\xi+\mu)^2+\eta^2, \\ \rho_2^2 &= (\xi+\mu-1)^2+\eta^2, \end{aligned} \tag{3}$$

$$n^2 = 1 + \frac{3}{2}A_1 - \frac{3}{2c^2}\left(1-\frac{\mu(1-\mu)}{3}\right), \tag{4}$$

where $0 < \mu \leq \frac{1}{2}$ is the ratio of the mass of the smaller primary to the total mass of the primaries, $\rho_1$andρ_2 are distances of the infinitesimal mass from the bigger and smaller primary, respectively; c is the velocity of light. A_1 characterizes the oblateness of the bigger primary and is given by $A_1 = \frac{AE^2-AP^2}{5R^2} << 1$ (McCuskey [23]) where AE and AP are the equatorial and polar radii of the bigger primary, and R is the distance between the primaries.

3 Locations of collinear points

Equilibrium points are those points at which no resultant force acts on the third infinitesimal body. Therefore, if it is placed at any of those points with zero velocity, it will stay there. In fact all derivatives of the coordinates with respect to the time are zero at these points.

$$W_\xi = 0 \quad \text{and} \quad W_\eta = 0, \tag{5}$$

W_ξ and W_η may be written as

$$W_\xi = \xi - \tfrac{(1-\mu)(\xi+\mu)}{\rho_1^3} - \tfrac{\mu(\xi-1+\mu)}{\rho_2^3} + \tfrac{3}{2}A_1\left\{\xi - \tfrac{(1-\mu)\,(\xi+\mu)}{\rho_1^5}\right\} + \tfrac{1}{c^2}\left[-3\xi\left\{1-\tfrac{\mu(1-\mu)}{3}\right\} + \tfrac{1}{2}\xi(\xi^2+\eta^2)\right.$$
$$-\tfrac{3}{2}(\xi^2+\eta^2)\left\{\tfrac{(1-\mu)(\xi+\mu)}{\rho_1^3} + \tfrac{\mu(\xi-1+\mu)}{\rho_2^3}\right\} + 3\left(\tfrac{1-\mu}{\rho_1}+\tfrac{\mu}{\rho_2}\right)\xi + \tfrac{(1-\mu)^2(\xi+\mu)}{\rho_1^4} + \tfrac{\mu^2(\xi-1+\mu)}{\rho_2^4}$$
$$+\mu(1-\mu)\left\{\tfrac{7}{2}\left(\tfrac{1}{\rho_1}-\tfrac{1}{\rho_2}\right) + \tfrac{7}{2}\xi\left(-\tfrac{(\xi+\mu)}{\rho_1^3} + \tfrac{(\xi-1+\mu)}{\rho_2^3}\right) + \tfrac{3}{2}\eta^2\left(\tfrac{\mu(\xi+\mu)}{\rho_1^5} + \tfrac{(1-\mu)(\xi-1+\mu)}{\rho_2^5}\right) + \tfrac{(\xi+\mu)}{\rho_1^3\rho_2}\right.$$
$$\left.+\tfrac{(\xi-1+\mu)}{\rho_1\rho_2^3} - \tfrac{(3\mu-2)\,(\xi+\mu)}{2\rho_1^3} - \tfrac{(1-3\mu)(\xi-1+\mu)}{2\rho_2^3}\right\} + A_1\left\{-\tfrac{9}{4}\left(1-\tfrac{\mu(1-\mu)}{3}\right)\xi + \tfrac{3}{2}(\xi^2+\eta^2)\xi\right.$$
$$+\left(-\tfrac{9(1-\mu)(\xi+\mu)}{4\rho_1^5} - \tfrac{9(1-\mu)(\xi+\mu)}{4\rho_1^3} - \tfrac{9\mu(\xi-1+\mu)}{4\rho_2^3}\right)(\xi^2+\eta^2) + \left(\tfrac{3(1-\mu)}{2\rho_1^3} + \tfrac{9(1-\mu)}{2\rho_1} + \tfrac{9\mu}{2\rho_2}\right)\xi$$
$$\left.+\tfrac{2(1-\mu)^2(\xi+\mu)}{\rho_1^6}\right\} + \mu(1-\mu)A_1\left\{\tfrac{7}{4\rho_1^3} + \tfrac{21}{4}\left(\tfrac{1}{\rho_1}-\tfrac{1}{\rho_2}\right) + \tfrac{7}{2}\xi\left(-\tfrac{3(\xi+\mu)}{2\rho_1^5}\right) + \tfrac{21}{4}\xi\left(-\tfrac{(\xi+\mu)}{\rho_1^3} + \tfrac{(\xi-1+\mu)}{\rho_2^3}\right)\right.$$
$$+\tfrac{9}{4}\eta^2\left(\tfrac{\mu(\xi+\mu)}{\rho_1^5} + \tfrac{(1-\mu)(\xi-1+\mu)}{\rho_2^5}\right) + \tfrac{3(1-\mu)(\xi+\mu)}{2\rho_1^5} + \tfrac{3(\xi+\mu)}{2\rho_1^3\rho_2} + \tfrac{3(\xi-1+\mu)}{2\rho_1\rho_2^3} - \tfrac{3\mu(\xi+\mu)}{4\rho_1^3}$$
$$\left.\left.-\tfrac{3(1-3\mu)(\xi-1+\mu)}{4\rho_2^3} + \tfrac{3(1-\mu)(\xi+\mu)}{2\rho_1^3}\right\}\right]$$

and

$$W_\eta = \eta\ F,$$

with

$$F = 1 - \tfrac{1-\mu}{\rho_1^3} - \tfrac{\mu}{\rho_2^3} + \tfrac{3}{2}A_1\left(1-\tfrac{1-\mu}{\rho_1^5}\right) + \tfrac{1}{c^2}\left[-3\left(1-\tfrac{\mu(1-\mu)}{3}\right) + \tfrac{1}{2}(\xi^2+\eta^2) - \tfrac{3}{2}(\xi^2+\eta^2)\left(\tfrac{1-\mu}{\rho_1^3}+\tfrac{\mu}{\rho_2^3}\right)\right.$$
$$+3\left(\tfrac{1-\mu}{\rho_1}+\tfrac{\mu}{\rho_2}\right) + \left(\tfrac{(1-\mu)^2}{\rho_1^4}+\tfrac{\mu^2}{\rho_2^4}\right) + \mu(1-\mu)\left\{\tfrac{7}{2}\xi\left(-\tfrac{1}{\rho_1^3}+\tfrac{1}{\rho_2^3}\right) - \left(\tfrac{\mu}{\rho_1^3}+\tfrac{1-\mu}{\rho_2^3}\right) + \tfrac{3}{2}\eta^2\left(\tfrac{\mu}{\rho_1^5}+\tfrac{(1-\mu)}{\rho_2^5}\right)\right.$$
$$\left.+\tfrac{1}{\rho_1^3\rho_2} + \tfrac{1}{\rho_1\rho_2^3} - \tfrac{(3\mu-2)}{2\rho_1^3} - \tfrac{(1-3\mu)}{2\rho_2^3}\right\} + A_1\left\{-\tfrac{9}{4}\left(1-\tfrac{\mu(1-\mu)}{3}\right) + \tfrac{3}{2}(\xi^2+\eta^2) + \left(\tfrac{-9(1-\mu)}{4\rho_1^5} - \tfrac{9(1-\mu)}{4\rho_1^3} - \tfrac{9\mu}{4\rho_2^3}\right)(\xi^2+\eta^2)\right.$$
$$\left.+\tfrac{3(1-\mu)}{2\rho_1^3} + \tfrac{9(1-\mu)}{2\rho_1} + \tfrac{9\mu}{2\rho_2} + \tfrac{2(1-\mu)^2}{\rho_1^6}\right\} + \mu(1-\mu)A_1\left\{\tfrac{21}{4}\ \xi\left(-\tfrac{1}{\rho_1^5} - \tfrac{1}{\rho_1^3} + \tfrac{1}{\rho_2^3}\right) - \tfrac{3}{2}\left(\tfrac{\mu}{\rho_1^3}+\tfrac{1-\mu}{\rho_2^3}\right) + \tfrac{9}{4}\eta^2\left(\tfrac{\mu}{\rho_1^5}+\tfrac{1-\mu}{\rho_2^5}\right)\right.$$
$$\left.\left.+\tfrac{3}{2}\left(\tfrac{(1-\mu)}{\rho_1^5} + \tfrac{1-\mu}{\rho_1^3} + \tfrac{1}{\rho_1^3\rho_2} + \tfrac{1}{\rho_1\rho_2^3} - \tfrac{\mu}{2\rho_1^3} - \tfrac{(1-3\mu)}{2\rho_2^3}\right)\right\}\right].$$

In order to find the collinear points, we put $\eta = 0$ in Eq.(5). The abscissa are the root of the equation.

$$f(\xi) = \xi - \tfrac{(1-\mu)(\xi+\mu)}{\rho_1} - \tfrac{\mu(\xi-1+\mu)}{\rho_2^3} + \tfrac{3}{2}A_1\left\{\xi - \tfrac{(1-\mu)\,(\xi+\mu)}{\rho_1^5}\right\} + \tfrac{1}{c^2}\left[-3\xi\left\{1-\tfrac{\mu(1-\mu)}{3}\right\} + \tfrac{1}{2}\xi^3\right.$$
$$-\tfrac{3}{2}\xi^2\left\{\tfrac{(1-\mu)(\xi+\mu)}{\rho_1^3} + \tfrac{\mu(\xi-1+\mu)}{\rho_2^3}\right\} + 3\left(\tfrac{1-\mu}{\rho_1}+\tfrac{\mu}{\rho_2}\right)\xi + \tfrac{(1-\mu)^2(\xi+\mu)}{\rho_1^4} + \tfrac{\mu^2(\xi-1+\mu)}{\rho_2^4}$$
$$+\mu(1-\mu)\left\{\tfrac{7}{2}\left(\tfrac{1}{\rho_1}-\tfrac{1}{\rho_2}\right) + \tfrac{7}{2}\xi\left(-\tfrac{(\xi+\mu)}{\rho_1^3} + \tfrac{(\xi-1+\mu)}{\rho_2^3}\right) + \tfrac{(\xi+\mu)}{\rho_1^3\rho_2} + \tfrac{(\xi-1+\mu)}{\rho_1\rho_2^3} - \tfrac{(3\mu-2)\,(\xi+\mu)}{2\rho_1^3}\right.$$
$$\left.-\tfrac{(1-3\mu)(\xi-1+\mu)}{2\rho_2^3}\right\} + A_1\left\{-\tfrac{9}{4}\left(1-\tfrac{\mu(1-\mu)}{3}\right)\xi + \tfrac{3}{2}\xi^3 + \left(-\tfrac{9(1-\mu)(\xi+\mu)}{4\rho_1^5} - \tfrac{9(1-\mu)(\xi+\mu)}{4\rho_1^3} - \tfrac{9\mu(\xi-1+\mu)}{4\rho_2^3}\right)\xi^2\right. \tag{6}$$
$$\left.+\left(\tfrac{3(1-\mu)}{2\rho_1^3} + \tfrac{9(1-\mu)}{2\rho_1} + \tfrac{9\mu}{2\rho_2}\right)\xi + \tfrac{2(1-\mu)^2(\xi+\mu)}{\rho_1^6}\right\} + \mu(1-\mu)A_1\left\{\tfrac{7}{4\rho_1^3} + \tfrac{21}{4}\left(\tfrac{1}{\rho_1}-\tfrac{1}{\rho_2}\right) + \tfrac{7}{2}\xi\left(-\tfrac{3(\xi+\mu)}{2\rho_1^5}\right)\right.$$
$$+\tfrac{21}{4}\xi\left(-\tfrac{(\xi+\mu)}{\rho_1^3} + \tfrac{(\xi-1+\mu)}{\rho_2^3}\right) + \tfrac{3(1-\mu)(\xi+\mu)}{2\rho_1^5} + \tfrac{3(\xi+\mu)}{2\rho_1^3\rho_2} + \tfrac{3(\xi-1+\mu)}{2\rho_1\rho_2^3} - \tfrac{3\mu(\xi+\mu)}{4\rho_1^3} - \tfrac{3(1-3\mu)(\xi-1+\mu)}{4\rho_2^3}$$
$$\left.\left.+\tfrac{3(1-\mu)(\xi+\mu)}{2\rho_1^3}\right\}\right] = 0$$

with $\rho_1 = |\xi+\mu|$, $\rho_2 = |\xi-1+\mu|$.
To locate the collinear points on the $\xi-$ axis, we divide the orbital plane into three parts: $\xi < \xi_1,\ \xi_1 < \xi < \xi_2$ and $\xi_2 < \xi$ with respect to the primaries where $\xi_1 = -\mu$ and $\xi_2 = 1-\mu$.

Case 1: Position of $L_1\ (\xi > \xi_2)$ (see Fig. 1 (a))
Let $\xi - \xi_2 = \lambda_1;\ \ \xi - \xi_1 = 1 + \lambda_1 \Rightarrow \xi = 1 + \lambda_1 + \xi_1$; since the distance between the primaries is unity, i.e. $\xi_2 - \xi_1 = 1$

$$\Rightarrow \xi_1 = -\mu\ \ and\ \ \xi_2 = 1-\mu\ \ then\ \ \xi = 1 + \lambda_1 - \mu;\ \rho_1 = 1 + \lambda;\ \rho_2 = \lambda_1. \tag{7}$$

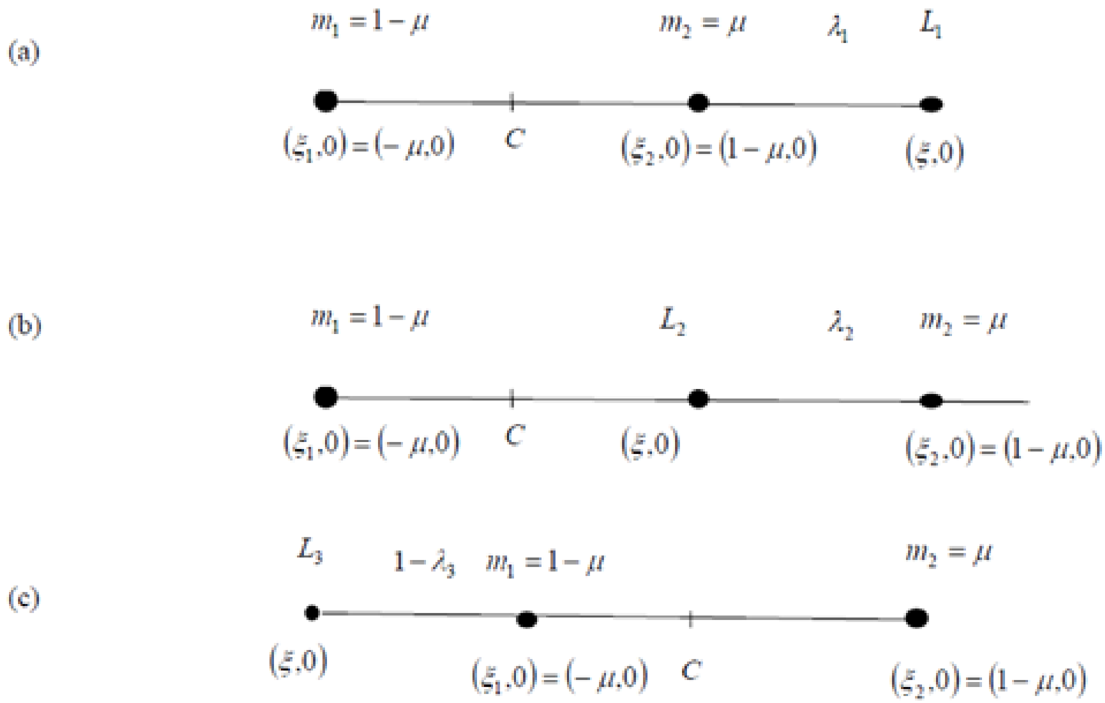

Figure 1: Reference parameter for collinear Lagrangian points.

Now substituting Eq.(7) in Eq.(6), we obtain

$$\begin{aligned}
&(2+6A_1)\,{\lambda_1}^{11} + (-18A_1\mu - 6\mu + 16 + 48A_1)\,{\lambda_1}^{10} + \big(44 - 38\mu - 123A_1\mu + 159A_1 + 15A_1\mu^2 \\
&+4c^2 + 6A_1c^2 + 2\mu^2\big)\,{\lambda_1}^{9} + \big(46 - 351A_1\,\mu + 291A_1 - 4\mu c^2 + 24c^2 + 36A_1c^2 + 2\mu^3 + 8\mu^2 \\
&-3A_1\mu^3 - 90\mu - 6A_1c^2\mu + 87A_1\mu^2\big)\,{\lambda_1}^{8} + \big(90A_1c^2 - 10 - 90\mu + 60c^2 + 10\mu^2 - 540A_1\mu \\
&+210A_1\mu^2 + 10\mu^3 - 30A_1\mu c^2 - 20\mu c^2 + 330A_1 - 15A_1\mu^3\big)\,{\lambda_1}^{7} + \big(76c^2 - 40\mu c^2 + 255A_1\mu^2 \\
&+120A_1c^2 - 30A_1\mu^3 - 68 - 462A_1\mu + 243A_1 + 20\mu^3 - 10\mu^2 - 60A_1c^2\mu\big)\,{\lambda_1}^{6} + \big(24\mu^3 + 90A_1c^2 \\
&+96\mu - 48\mu c^2 + 116A_1\mu^2 - 60 + 114A_1 - 56\mu^2 - 24A_1\mu^3 - 60A_1c^2\mu - 161A_1\mu + 48c^2\big)\,{\lambda_1}^{5} \\
&+\big(126\mu - 24A_1c^2\mu - 92A_1\mu^2 + 98A_1\mu + 12c^2 - 48\mu c^2 + 30A_1c^2 + 30A_1 + 24\mu^3 - 94\mu^2 - 18\big)\,{\lambda_1}^{4} \\
&+\big(11A_1 + 102\mu + 135A_1\mu + 20\mu^3 - 76\mu^2 + 18A_1\mu^3 - 155A_1\mu^2 - 40\mu c^2\big)\,{\lambda_1}^{3} + (75A_1\mu + 50\mu \\
&-20\mu c^2 - 20\mu^2 + 15A_1\mu^3 + 10\mu^3 - 90A_1\mu^2\big)\,{\lambda_1}^{2} + \big(-4\mu c^2 + 8\mu^2 - 18A_1\mu^2 + 10\mu \\
&+3A_1\mu^3 + 15A_1\mu + 2\mu^3\big)\,\lambda_1 + 4\mu^2 = 0.
\end{aligned} \tag{8}$$

In the presence of oblateness only, we have

$$\begin{aligned}
&(3A_1+2)\,\lambda_1^7 + (-2\mu + 10 - 3A_1\mu + 15A_1)\,\lambda_1^6 + (-8\mu - 12A_1\mu + 20 + 30A_1)\,\lambda_1^5 + (-12\mu - 18A_1\mu + 18 \\
&30A_1)\,\lambda_1^4 + (15A_1 - 12A_1\mu + 6 - 12\mu)\,\lambda_1^3 - 12\mu\lambda_1^2 - 8\mu\lambda_1 - 2\mu = 0.
\end{aligned} \tag{8a}$$

Case 2: Position of $L_2\,(\xi_1 < \xi < \xi_2)$ (see Fig. 1 (b))

$$Let\;\; \xi_2 - \xi = \lambda_2;\;\; \xi - \xi_1 = 1 - \lambda_2 \Rightarrow \xi = 1 - \lambda_2 - \mu;\, \rho_1 = 1 - \lambda_2;\, \rho_2 = \lambda_2. \tag{9}$$

Substituting Eq.(9) in Eq.(6), we obtain

$$\begin{aligned}&(2+6A_1)\,{\lambda_2}^{11}+(18A_1\mu+6\mu-48A_1-16)\,{\lambda_2}^{10}+\left(15A_1\mu^2+159A_1+2\mu^2-38\mu+4c^2+44\right.\\&\left.-123A_1\mu+6A_1c^2\right){\lambda_2}^{9}+\left(-8\mu^2+6A_1c^2\mu-36A_1c^2+102\mu+369A_1\mu-87A_1\mu^2-46-24c^2\right.\\&\left.-291A_1+3A_1\mu^3-2\mu^3+4\mu c^2\right){\lambda_2}^{8}+\left(-630A_1\mu+10\mu^3+210A_1\mu^2-30A_1\mu c^2+90A_1c^2\right.\\&\left.+60c^2+330A_1-150\mu-15A_1\mu^3-10+10\mu^2-20\mu c^2\right){\lambda_2}^{7}+\left(132\mu-16\mu^3-279A_1\mu^2\right.\\&\left.+36A_1\mu^3-76c^2-6\mu^2-120A_1c^2+660A_1\mu+68-243A_1+60A_1c^2\mu+32\mu c^2\right){\lambda_2}^{6}\\&+\left(-100\mu-455A_1\mu+4\mu^3+40\mu^2+260A_1\mu^2-54A_1\mu^3+114A_1-60-60A_1c^2\mu+90A_1c^2\right.\\&\left.+48c^2-8\mu c^2\right){\lambda_2}^{5}+\left(256A_1\mu+16\mu^3-30A_1c^2-122\mu^2+60A_1\mu^3-12c^2+24A_1c^2\mu\right.\\&\left.-232A_1\mu^2-30A_1+18+110\mu-32\mu c^2\right){\lambda_2}^{4}+\left(-20\mu^3-171A_1\mu-102\mu+156\mu^2-42A_1\mu^3\right.\\&\left.+193A_1\mu^2 40\mu c^2+11A_1\right){\lambda_2}^{3}+\left(-90A_1\mu^2+10\mu^3+50\mu+75A_1\mu+15A_1\mu^3\right.\\&\left.-100\mu^2-20\mu c^2\right){\lambda_2}^{2}+\left(18A_1\mu^2-15A_1\mu-3A_1\mu^3+32\mu^2-10\mu-2\mu^3+4\mu c^2\right)\lambda_2-4\mu^2=0.\end{aligned} \tag{10}$$

In the presence of oblateness effect only, we have

$$\begin{aligned}&(-3A_1-2)\,\lambda_2^7+(-2\mu+10-3A_1\mu+15A_1)\,\lambda_2^6+(8\mu+12A_1\mu-20-30A_1)\,\lambda_2^5+(-8\mu-18A_1\mu+18\\&+30A_1)\,\lambda_2^4+(-15A_1+12A_1\mu-6-4\mu)\,\lambda_2^3+12\mu\lambda_2^2-8\mu\lambda_1+2\mu=0.\end{aligned} \tag{10a}$$

Case 3: Position of L_3 $(\xi<\xi_1)$ (see Fig. 1 (c))
Let the distance of the point L_3 from the bigger primary be $1-\lambda_3$.

$$Since\ \ \xi_2-\xi_1=1\Rightarrow\xi_1-\xi=1-\lambda_3;\ \xi_2-\xi=2-\lambda_3\ \ and\ \ \xi=\lambda_3-\mu-1;\ \ \rho_1=1-\lambda_3;\ \ \rho_2=2-\lambda_3. \tag{11}$$

Substituting Eq.(11) in Eq.(6), we obtain

$$\begin{aligned}&(2+6A_1)\,{\lambda_3}^{11}+(-18A_1\mu-6\mu-28-84A_1)\,{\lambda_3}^{10}+\left(164+4c^2+82\mu+519A_1+2\mu^2+6A_1c^2\right.\\&\left.+15A_1\mu^2+237A_1\mu\right){\lambda_3}^{9}+\left(-72A_1c^2-4\mu c^2-6A_1c^2\mu-486\mu-518-28\mu^2-48c^2-1869A_1\right.\\&\left.-3A_1\mu^3+2\mu^3-1377A_1\mu-183A_1\ \mu^2\right){\lambda_3}^{8}+\left(44\mu c^2+922+33A_1\mu^3-22\mu^3+1638\mu+378A_1c^2\right.\\&\left.+252c^2+170\mu^2+66A_1c^2\mu+4644A_1\mu+4368A_1+978A_1\mu^2\right){\lambda_3}^{7}+\left(-578\mu^2-208\mu c^2\right.\\&-6987A_1-3464\mu-1140A_1c^2-10074A_1\mu-776-156A_1\mu^3-312A_1\mu\, c^2-756c^2+104\mu^3\\&\left.-2991\mu^2A_1\right){\lambda_3}^{6}+\left(1204\mu^2+5734A_1\mu^2+7860A_1-280\mu^3+4788\mu+14747A_1\mu+828A_1c^2\mu\right.\\&\left.+408A_1\mu^3-220+560\mu\, c^2+1416c^2+2178A_1c^2\right){\lambda_3}^{5}+\left(-2730A_1c^2-1356A_1c^2\mu+476\mu^3\right.\\&\left.-14914A_1\mu-6270A_1-952\mu c^2-1586\mu^2-630A_1\mu^3-4362\mu-7082A_1\mu^2-1692c^2+1274\right){\lambda_3}^{4}\\&+\left(-1372+2550\mu+1428A_1c^2\mu+1056\mu\, c^2+1256c^2+2220A_1c^2+5559A_1\mu^2-528\mu^3+10513A_1\mu\right.\\&\left.+552A_1\mu^3+3503A_1+1320\mu^2\right){\lambda_3}^{3}+(696-1080\ A_1c^2-5077A_1\mu-862\mu-676\mu^2-528c^2\\&-2636A_1\mu^2-1338A_1-984A_1c^2\mu+374\mu^3-748c^2\mu-207A_1\mu^3\big){\lambda_3}^{2}+(1493\ A_1\mu-154\mu^3\\&+706A_1\mu^2+200\mu^2-144+240A_1c^2+372A_1+308\mu c^2-39A_1\mu^3+110\mu+432A_1c^2\mu+96c^2\big)\,\lambda_3\\&+\left(12\mu-88A_1+28\mu^3-96A_1c^2\mu-158A_1\mu+42A_1\mu^3-108A_1\mu^2-28\mu^2\ -56\mu c^2\right)=0.\end{aligned} \tag{12}$$

In the presence of oblateness effect only, we have

$$\begin{aligned}&(3A_1+2)\,\lambda_3^7+(-2\mu-18-3A_1\mu-27A_1)\,\lambda_3^6+(16\mu+24A_1\mu+68+102A_1)\,\lambda_3^5+(-52\mu-78A_1\mu-138\\&-210A_1)\,\lambda_3^4+(225A_1+132A_1\mu+92\mu+158)\,\lambda_3^3+(-180A_1-126A_1\mu-96\mu-96)\,\lambda_3^2+(60A_1+72A_1\mu\\&+56\mu+24)\,\lambda_3-14\mu-24A_1\mu=0.\end{aligned} \tag{12a}$$

It is noticed that in each case there exists only one physically reasonable root.

4 Stability of collinear points

We examine the stability of an equilibrium configuration that is its ability to restrain the body motion in its vicinity. To do so we displace the infinitesimal body a little from an equilibrium point with small velocity. If its motion is rapid departure from vicinity of the point, we call such a position of equilibrium an unstable one. If the body oscillates about the point, it is said to be a stable position.

In order to study the stability of the collinear points, following Singh and Bello [12, 13], the characteristic equation is given by

$$(P_1q_2 - P_2q_1)\lambda^4 + (P_1q_6 + P_5q_2 + P_3q_4 - P_6q_1 - P_2q_5 - P_4q_3)\lambda^2 + P_5q_6 - P_6q_5 = 0, \tag{13}$$

where

$$\begin{gathered} P_1 = 1 + W^0_{\dot\xi\dot\xi}, P_2 = W^0_{\dot\eta\dot\xi}, P_3 = W^0_{\xi\dot\xi} - W^0_{\xi\dot\xi} = 0, P_4 = \left\{W^0_{\eta\dot\xi} - 2n - W^0_{\xi\dot\eta},\right\} \\ P_5 = -W^0_{\xi\xi}, P_6 = -W^0_{\xi\eta}, q_1 = W^0_{\dot\xi\dot\eta}, q_2 = 1 + W^0_{\dot\eta\dot\eta}, q_3 = 2n + W^0_{\xi\dot\eta} - W^0_{\eta\dot\xi}, \\ q_4 = W^0_{\eta\dot\eta} - W^0_{\eta\dot\eta} = 0, q_5 = -W^0_{\xi\eta}, q_6 = -W^0_{\eta\eta}. \end{gathered}$$

The second order partial derivatives of W are denoted by subscripts. The superscripts 0 indicates that the derivative is to be evaluated at the equilibrium points (ξ_0, η_0) where

$$\begin{aligned} &W^0_{\xi\xi} = 1 + \tfrac{3(1-\mu)(\xi+\mu)^2}{\rho_1^5} - \tfrac{(1-\mu)}{\rho_1^3} + \tfrac{3\mu(\xi-1+\mu)^2}{\rho_2^5} - \tfrac{\mu}{\rho_2^3} + A_1\left\{\tfrac{3}{2} + \tfrac{15(1-\mu)(\xi+\mu)^2}{2\rho_1^7} - \tfrac{3(1-\mu)}{2\rho_1^5}\right\} + \\ &\tfrac{1}{c^2}\Big[(\mu(1-\mu)-3) + \tfrac{3}{2}\xi^2 + \left(\tfrac{9(1-\mu)(\xi+\mu)^2}{2\rho_1^5} - \tfrac{3(1-\mu)}{2\rho_1^3} - \tfrac{3\mu}{2\rho_2^3} + \tfrac{9\mu(\xi-1+\mu)^2}{2\rho_2^5}\right)\xi^2 + 2\Big(\tfrac{-3(1-\mu)(\xi+\mu)}{\rho_1^3} \\ &-\tfrac{3\mu(\xi-1+\mu)}{\rho_2^3}\Big)\xi + \tfrac{3(1-\mu)}{\rho_1} + \tfrac{3\mu}{\rho_2} - \tfrac{4(1-\mu)^2(\xi+\mu)^2}{\rho_1^6} + \tfrac{(1-\mu)^2}{\rho_1^4} - \tfrac{4\mu^2(\xi-1+\mu)^2}{\rho_2^6} + \tfrac{\mu^2}{\rho_2^4} + \mu(1-\mu)\Big\{\Big(-\tfrac{7(\xi+\mu)}{\rho_1^3} \\ &+\tfrac{7(\xi-1+\mu)}{\rho_2^3}\Big) + \tfrac{7}{2}\xi\left(\tfrac{3(\xi+\mu)^2}{\rho_1^5} - \tfrac{1}{\rho_1^3} + \tfrac{1}{\rho_2^3} - \tfrac{3(\xi-1+\mu)^2}{\rho_2^5}\right) - \tfrac{3(\xi+\mu)^2}{\rho_1^5\rho_2} - \tfrac{2(\xi+\mu)(\xi-1+\mu)}{\rho_1^3\rho_2^3} + \tfrac{1}{\rho_1^3\rho_2} - \tfrac{3(\xi-1+\mu)^2}{\rho_1\rho_2^5} \\ &+\tfrac{1}{\rho_1\rho_2^3} + \tfrac{3(3\mu-2)(\xi+\mu)^2}{2\rho_1^5} - \tfrac{(3\mu-2)}{2\rho_1^3} - \tfrac{(1-3\mu)}{2\rho_2^3} + \tfrac{3(1-3\mu)(\xi-1+\mu)^2}{2\rho_2^5}\Big\} \\ &+A_1\Big\{\tfrac{3}{4}(\mu(1-\mu)-3) + \tfrac{9}{2}\xi^2 + \tfrac{3}{4}\xi^2\left(\tfrac{9(1-\mu)(\xi+\mu)^2}{\rho_1^5} - \tfrac{3(1-\mu)}{\rho_1^3} - \tfrac{3\mu}{\rho_2^3} + \tfrac{9\mu(\xi-1+\mu)^2}{\rho_2^5}\right) + \Big(\tfrac{45(1-\mu)(\xi+\mu)^2}{4\rho_1^7} \\ &-\tfrac{9(1-\mu)}{\rho_1^5}\Big)\xi^2 + 3\xi\left(-\tfrac{3(1-\mu)(\xi+\mu)}{\rho_1^3} - \tfrac{3\mu(\xi-1+\mu)}{\rho_2^3}\right) - \tfrac{9(1-\mu)(\xi+\mu)}{\rho_1^5}\xi + \left(\tfrac{9(1-\mu)}{2\rho_1} + \tfrac{9\mu)}{2\rho_2} + \tfrac{3(1-\mu)}{2\rho_1^3}\right) \\ &-\tfrac{16(1-\mu)^2(\xi+\mu)^2}{\rho_1^8} + \tfrac{2(1-\mu)^2}{\rho_1^6}\Big\} + \mu(1-\mu)A_1\Big\{\tfrac{-21}{2}\left(\tfrac{\xi+\mu}{\rho_1^5} + \tfrac{\xi+\mu}{\rho_1^3} - \tfrac{(\xi-1+\mu)}{\rho_2^3}\right) + \tfrac{7}{2}\xi\left(\tfrac{15(1-\mu)^2}{2\rho_1^7} - \tfrac{3}{2\rho_1^5}\right) \\ &+\tfrac{21}{4}\xi\left(\tfrac{3(\xi+\mu)^2}{\rho_1^5} - \tfrac{1}{\rho_1^3} + \tfrac{1}{\rho_2^3} - \tfrac{3(\xi-1+\mu)^2}{\rho_2^5}\right) - \tfrac{15(1-\mu)(\xi+\mu)^2}{2\rho_1^7} + \tfrac{3(1-\mu)}{2\rho_1^5} - \tfrac{9(\xi+\mu)^2}{2\rho_1^5\rho_2} - \tfrac{3(\xi+\mu)(\xi-1+\mu)^2}{\rho_1^3\rho_2^3} \\ &+\tfrac{3}{2\rho_1^3\rho_2} + \tfrac{3}{2\rho_1\rho_2^3} - \tfrac{9(\xi-1+\mu)^2}{2\rho_1\rho_2^5} + \tfrac{9(3\mu-2)(\xi+\mu)^2}{4\rho_1^5} - \tfrac{3(3\mu-2)}{4\rho_1^3} - \tfrac{3(1-3\mu)}{4\rho_2^3} + \tfrac{9(1-3\mu)(\xi-1+\mu)^2}{4\rho_2^5}\Big\}\Big], \end{aligned} \tag{14}$$

$$\begin{aligned} &W^0_{\eta\eta} = 1 - \tfrac{(1-\mu)}{\rho_1^3} - \tfrac{\mu}{\rho_2^3} + A_1\left\{\tfrac{3}{2} - \tfrac{3(1-\mu)}{2\rho_1^5}\right\} + \tfrac{1}{c^2}\Big[(\mu(1-\mu)-3) + \tfrac{3}{2}\xi^2 + \left(-\tfrac{3(1-\mu)}{2\rho_1^3} - \tfrac{3\mu}{2\rho_2^3}\right)\xi^2 + \tfrac{3(1-\mu)}{\rho_1} + \tfrac{3\mu}{\rho_2} \\ &+\tfrac{(1-\mu)^2}{\rho_1^4} + \tfrac{\mu^2}{\rho_2^4} + \mu(1-\mu)\left\{\tfrac{7}{2}\xi\left(-\tfrac{1}{\rho_1^3} + \tfrac{1}{\rho_2^3}\right) - \tfrac{\mu}{\rho_1^3} - \tfrac{(1-\mu)}{\rho_2^3} + \tfrac{1}{\rho_1^3\rho_2} + \tfrac{1}{\rho_1\rho_2^3} - \tfrac{(3\mu-2)}{2\rho_1^3} - \tfrac{(1-3\mu)}{2\rho_2^3}\right\} \\ &+A_1\left\{\tfrac{3}{4}(\mu(1-\mu)-3) + \tfrac{3}{2}\xi^2 + \tfrac{3}{2}\xi^2\left(-\tfrac{3(1-\mu)}{2\rho_1^3} - \tfrac{3\mu}{2\rho_2^3}\right) - \tfrac{9(1-\mu)}{4\rho_1^5}\xi^2 + \tfrac{9(1-\mu)}{2\rho_1} + \tfrac{9\mu}{2\rho_2} + \tfrac{3(1-\mu)}{2\rho_1^3} + \tfrac{2(1-\mu)^2}{\rho_1^6}\right\} \\ &+\mu(1-\mu)A_1\left\{-\tfrac{21\xi}{4\rho_1^5} + \tfrac{21\xi}{4}\left(-\tfrac{1}{\rho_1^3} + \tfrac{1}{\rho_2^3}\right) - \tfrac{3\mu}{2\rho_1^3} - \tfrac{3(1-\mu)}{2\rho_2^3} + \tfrac{3(1-\mu)}{2\rho_1^5} + \tfrac{3}{2\rho_1^3\rho_2} + \tfrac{3}{2\rho_1\rho_2^3} - \tfrac{3(3\mu-2)}{4\rho_1^3} - \tfrac{3(1-3\mu)}{4\rho_2^3}\right\}\Big], \end{aligned} \tag{15}$$

$$W^0_{\xi\eta} = 0, \tag{16}$$

$$W^0_{\dot\xi\dot\xi} = \tfrac{1}{c^2}\left[\tfrac{1}{2}\xi^2 + \tfrac{3(1-\mu)}{\rho_1} + \tfrac{3\mu}{\rho_2} + A_1\left(\tfrac{3}{2}\xi^2 + \tfrac{3(1-\mu)}{2\rho_1^3}\right)\right], \tag{17}$$

$$W^0_{\dot\eta\dot\eta} = \tfrac{1}{c^2}\left[\tfrac{3}{2}\xi^2 + \tfrac{3(1-\mu)}{\rho_1} + \tfrac{3\mu}{\rho_2} + A_1\left(\tfrac{9}{4}\xi^2 + \tfrac{3(1-\mu)}{2\rho_1^3}\right)\right], \tag{18}$$

$$W^0_{\dot\eta\dot\xi} = 0, \tag{19}$$

$$W^0_{\xi\dot\xi} = 0, \tag{20}$$

$$W^0_{\eta\dot\eta} = 0, \tag{21}$$

$$\begin{aligned} W^0_{\xi\dot\eta} = \tfrac{1}{c^2}\Big\{&\tfrac{3}{2}\xi^2 + \tfrac{3(1-\mu)}{\rho_1} + \tfrac{3\mu}{\rho_2} + \left(-\tfrac{3(1-\mu)(\xi+\mu)}{\rho_1^3} - \tfrac{3\mu(\xi+\mu-1)}{\rho_2^3}\right)\xi + 4\mu(1-\mu)\left(-\tfrac{(\xi+\mu)}{\rho_1^3} + \tfrac{(\xi+\mu-1)}{\rho_2^3}\right) \\ &+ \Big[\tfrac{27}{8}\xi^2 + \tfrac{9(1-\mu)}{4\rho_1} + \tfrac{9\mu}{4\rho_2} + \tfrac{3(1-\mu)}{2\rho_1^3} + \left(-\tfrac{9(1-\mu)(\xi+\mu)}{4\rho_1^3} - \tfrac{9\mu(\xi+\mu-1)}{4\rho_2^3} - \tfrac{9(1-\mu)(\xi+\mu)}{2\rho_1^5}\right)\xi \\ &+ 4\mu(1-\mu)\left(-\tfrac{3(\xi+\mu)}{2\rho_1^5}\right) + 3\mu(1-\mu)\left(-\tfrac{(\xi+\mu)}{\rho_1^3} + \tfrac{(\xi+\mu-1)}{\rho_2^3}A_1\right)\Big]\Big\}, \end{aligned} \tag{22}$$

$$W^0_{\eta\dot\xi} = \tfrac{1}{c^2}\left\{-\tfrac{1}{2}\xi^2 - \tfrac{3(1-\mu)}{\rho_1} - \tfrac{3\mu}{\rho_2} + \left[-\tfrac{9}{8}\xi^2 - \tfrac{9(1-\mu)}{4\rho_1} - \tfrac{3(1-\mu)}{2\rho_1^3} - \tfrac{9\mu}{4\rho_2}\right]A_1\right\}, \tag{23}$$

Table 1: Parameters of the system.

S/No	System	μ	c	A_1
1	Jupiter-Io	0.0000415622	17294.81937	0.0006885582
1	Jupiter-Io	0.0000415622	17294.81937	0.0006885582
2	Jupiter-Europa	0.00002526534711	21817.21721	0.0002717680
3	Saturn-Mimas	0.0000000668	20967.08625	0.0038673922
4	Saturn-Thethy	0.0000011421	26424.27518	0.0015345696

Table 2: Positions of the collinear equilibrium points.

S/No. of the system	L_1	L_2	L_3
1	1.024166773125	0.976134628032	-1.000017317589
	1.024153112270	0.976225653150	-1.000017330678
	1.024153112240	0.976148508290	-1.000041562200
	1.024166770550	0.976134630550	-1.000041562200
2	1.020425563162	0.979799229733	-1.000010478409
	1.020420999940	0.979803855220	-1.000010481547
	1.020420999920	0.979803855230	-1.000025148200
	1.020425567970	0.979799225010	-1.000025148200
3	1.002815442311	0.997189698986	-1.000000027820
	1.002806883664	0.997198275690	-1.000000027951
	1.002806883659	0.997197674490	-1.000000066800
	1.002815884274	0.997188657415	-1.000000066800
4	1.007263912707	0.992768821174	-1.000000475872
	1.007255780406	0.992778073121	-1.000000476675
	1.007254705102	0.992768073124	-1.000001142100
	1.007263927812	0.992768806203	-1.000001142100

5 Numerical results

We have used the above mentioned analysis to calculate the locations and stability of the collinear points of Jupiter – Satellite and Saturn-Satellite. The necessary data have been borrowed from Sharma and SubbaRao [2], and Murray and Dermott [24]. The mass parameter (μ), the oblateness coefficient (A_1) and the dimensionless speed of light (c) of the systems consisting of a major planet and its satellite have been presented in Table 1. It should be noted here that, the oblateness effect of the bigger primary only is considered. In Table 2, the corresponding positions in the classical problem, classical problem with oblateness, relativistic problem, and relativistic problem with oblateness respectively for comparison purposes (first entry, second entry, third entry and fourth entry for each system) have been presented.

6 Discussion

Eqs.(1)-(4) describe the motion of a third body under the influence of the oblateness of the bigger primary and relativistic factor. Eqs.(8), (10), and (12) give respective locations of the collinear equilibrium points L_1, L_2, and L_3 in the presence of relativistic and oblateness factors while equations (8a), (10a), and (12a) give their locations in the presence of oblateness factor only.

A numerical analysis of the positions of the collinear points $L_i(i = 1,\ 2,\ 3)$ shows that: the oblateness effect and relativistic effect, all cause a shift of L_1 towards the smaller primary for each system as shown in Table 2; similarly the oblateness effect and relativistic effect, cause a shift of L_2 towards the smaller primary for each system as shown in Table 2; also L_3 moves away from the bigger primary due to the effect of oblateness (by comparing the 1^{st} and 3^{rd} entries of Table 2 for each system), while the effect of oblateness from the 3^{rd} and 4^{th} entries of Table 2 for each system does not show physically (up to 12 decimal places) a significant effect in the presence of relativistic term on L_3 for each system. Also when varying the mass ratio μ, it is observed graphically that: the position of L_1 for each system moves away from the smaller primary as mass ratio μ increases. It is seen that, the four graphs of L_1 of each figure for each system

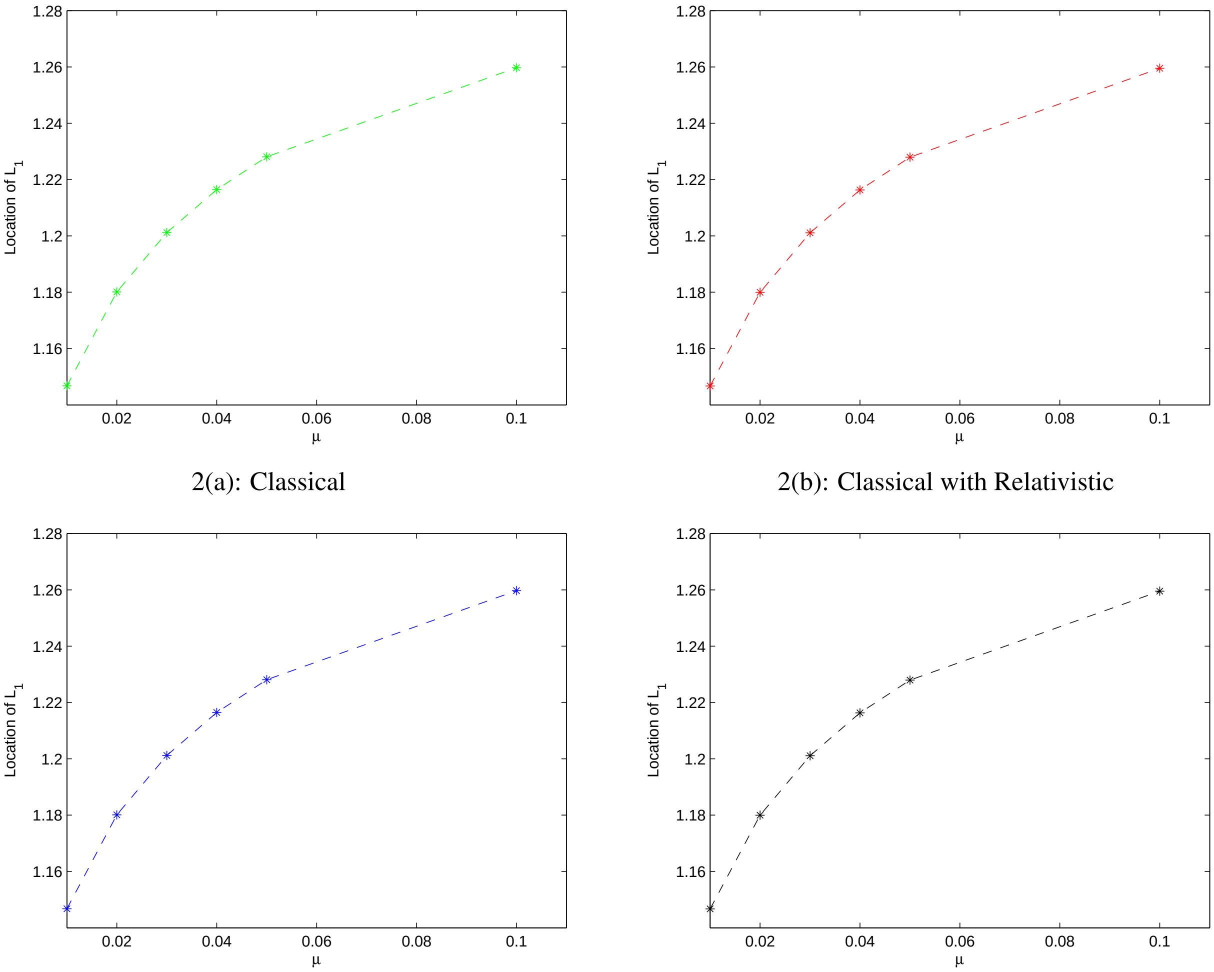

2(a): Classical

2(b): Classical with Relativistic

2(c): Classical

2(d): Classical with Relativistic

Figure 2: Position of L_1 with varying mass ratio of Jupiter-IO.

Table 3: Stability of L_1.

	Jupiter-IO	Jupiter-Europa	Saturn-Mimas	Saturn-Thety
P_1	1.0000000115698	1.00000000727933	1.00000000797525	1.00000000499931
P_2	0	0	0	0
P_3	0	0	0	0
P_4	-2.00103284434348	-2.00040765638627	-2.00580109292184	-2.00230185731859
P_5	-8.73527282189395	-8.76805140392746	-9.05284263324122	-8.94783630934580
P_6	0	0	0	0
q_1	0	0	0	0
q_2	1.00000001507830	1.00000000946747	1.00000001026938	1.00000000645400
q_3	2.00103284434348	2.00040765638627	2.00580109292184	2.00230185731859
q_4	0	0	0	0
q_5	0	0	0	0
q_5	2.86517073449440	2.88304588298070	3.01199934173697	2.96824524932270
$\omega_{1,3}$	$\pm$2.45398503036729	$\pm$2.46107837126842	$\pm$2.51538304471107	$\pm$2.49641546398785
$\omega_{2,4}$	$\pm 2.03864485312412i$	$\pm 2.04292241404883i$	$\pm 2.07594473971419i$	$\pm 2.06439139125632i$

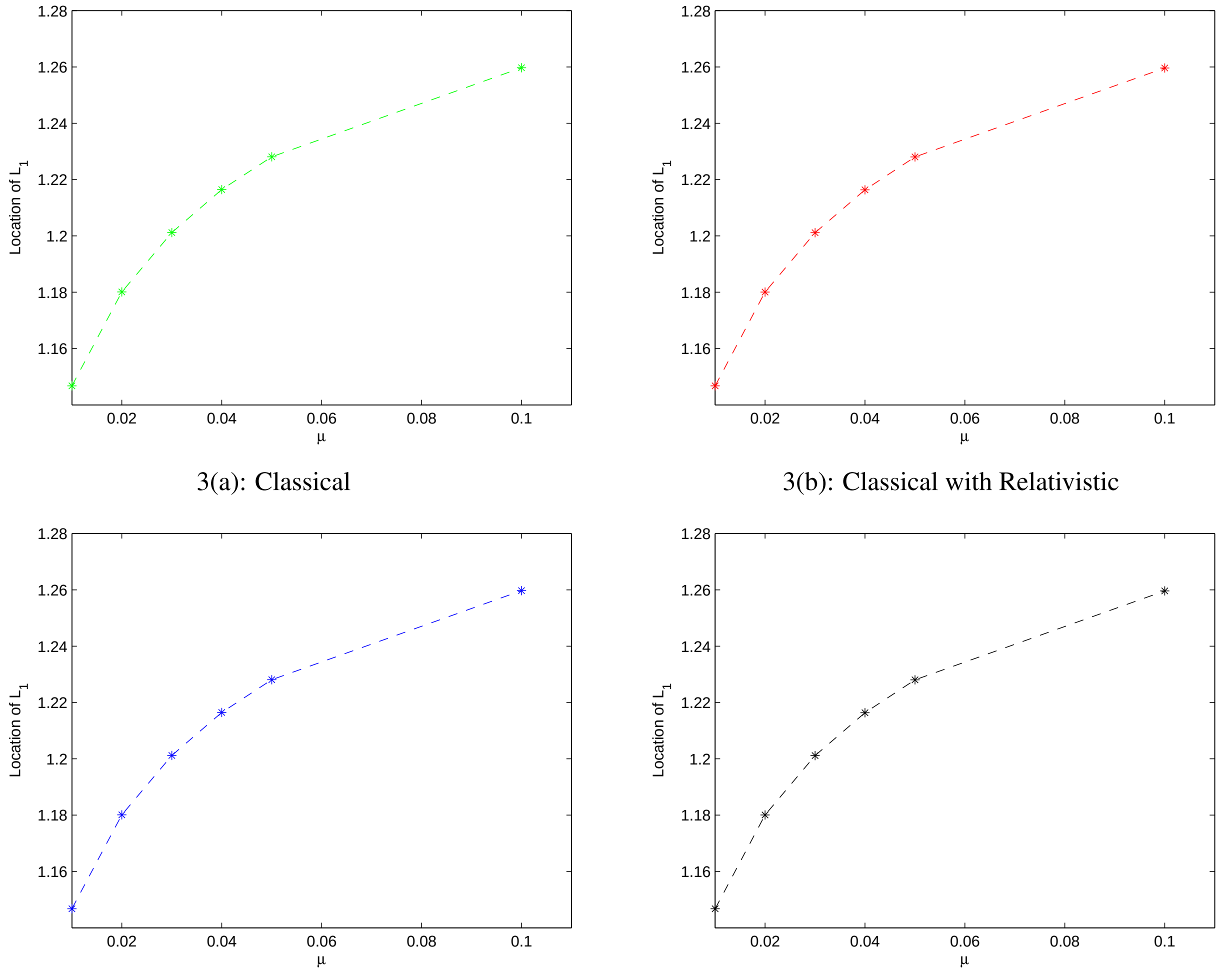

3(a): Classical

3(b): Classical with Relativistic

3(c): Classical

3(d): Classical with Relativistic

Figure 3: Position of L_1 with varying mass ratio of Jupiter-Europa.

Table 4: Stability of L_2.

	Jupiter-IO	Jupiter-Europa	Saturn-Mimas	Saturn-Thety
P_1	1.0000000118928	1.00000000745041	1.00000000800084	1.00000000504082
P_2	0	0	0	0
P_3	0	0	0	0
P_4	-2.00103284369928	-2.00040765604394	-2.00580109286977	-2.00230185723499
P_5	-9.31375179654457	-9.25852351359258	-9.12144809636026	-9.12290146470277
P_6	0	0	0	0
q_1	0	0	0	0
q_2	1.00000001507858	1.00000000946758	1.00000001026938	1.00000000645400
q_3	2.00103284369928	2.00040765604394	2.00580109286977	2.00230185723499
q_4	0	0	0	0
q_5	0	0	0	0
q_5	3.15416161414424	3.12819885574388	3.04613938687089	3.05561116824838
$\omega_{1,3}$	$\pm$2.56980561735547	$\pm$2.55934925721325	$\pm$2.52905776064064	$\pm$2.53143465465686
$\omega_{2,4}$	$\pm$2.10913326401056i	$\pm$2.10275408085974i	$\pm$2.08424145422663i	$\pm$2.08568545615364i

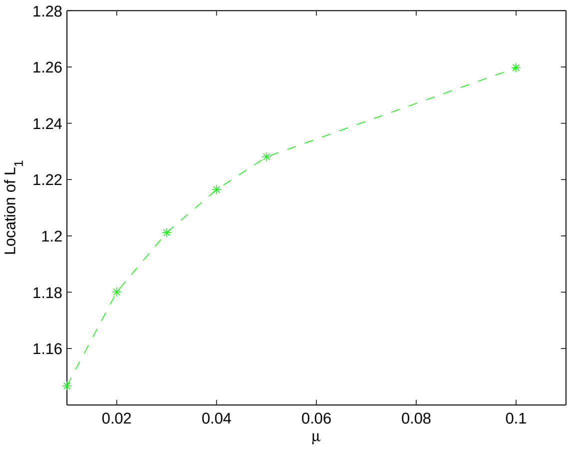

4(a): Classical

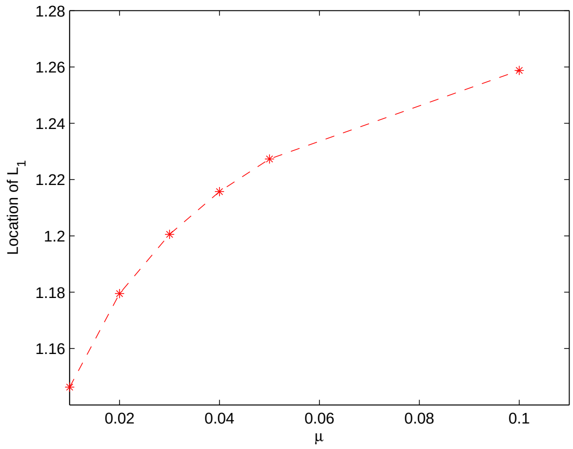

4(b): Classical with Relativistic

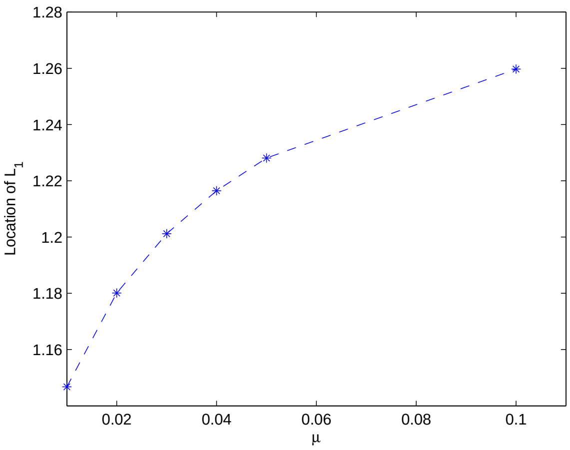

4(c): Classical

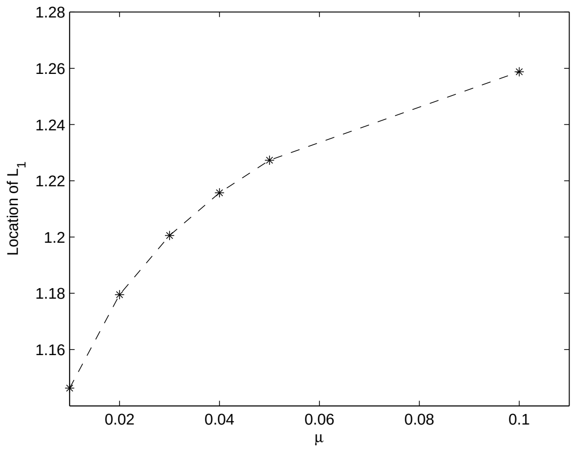

4(d): Classical with Relativistic

Figure 4: Position of L_1 with varying mass ratio of Saturn-Mimas.

Table 5: Stability of L_3.

	Jupiter-IO	Jupiter-Europa	Saturn-Mimas	Saturn-Thety
P_1	1.00000001187233	1.00000000744199	1.00000000800068	1.00000000504013
P_2	0	0	0	0
P_3	0	0	0	0
P_4	-2.00103284392922	-2.00040765616702	-2.00580109288902	-2.00230185726575
P_5	-3.15380732278084	-3.12739402170511	-3.04623511053352	-3.05575984541978
P_6	0	0	0	0
q_1	0	0	0	0
q_2	1.00000001506191	1.00000000946003	1.00000001026921	1.00000000645334
q_3	2.00103284392922	2.00040765616702	2.00580109288902	2.00230185726575
q_4	0	0	0	0
q_5	0	0	0	0
q_5	0.0741909411575225	0.0626344715841146	0.00853289933225515	0.0220404413814476
$\omega_{1,3}$	$\pm$0.45477550578882	$\pm$0.419539571565593	$\pm$0.160325603462717	$\pm$0.254450506724606
$\omega_{2,4}$	$\pm 1.06364314974664i$	$\pm 1.05493348031331i$	$\pm 1.00560432722787i$	$\pm 1.01990275825692i$

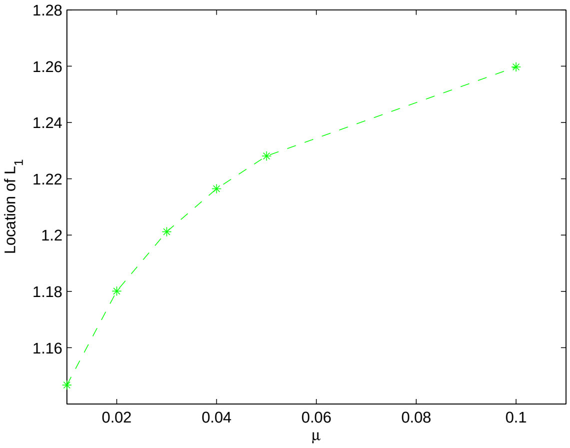

5(a): Classical

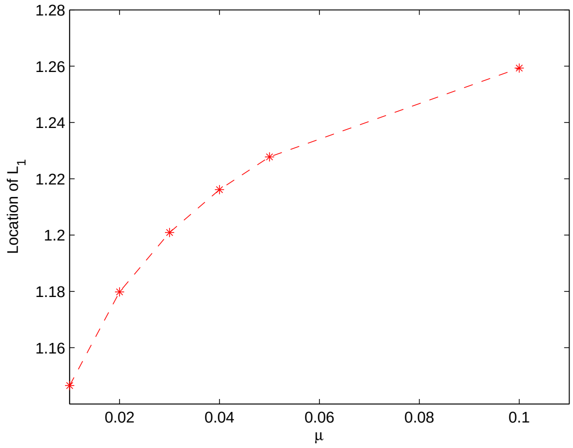

5(b): Classical with Relativistic

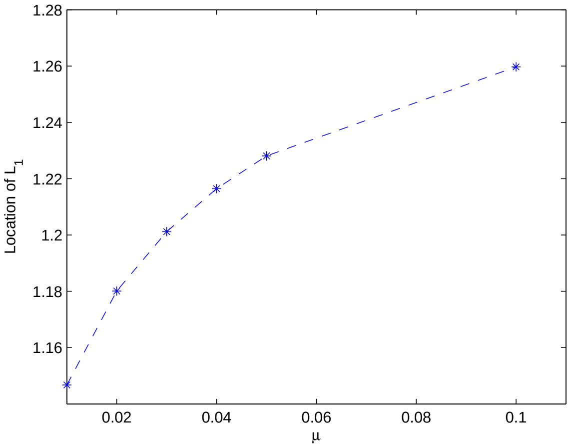

5(c): Classical

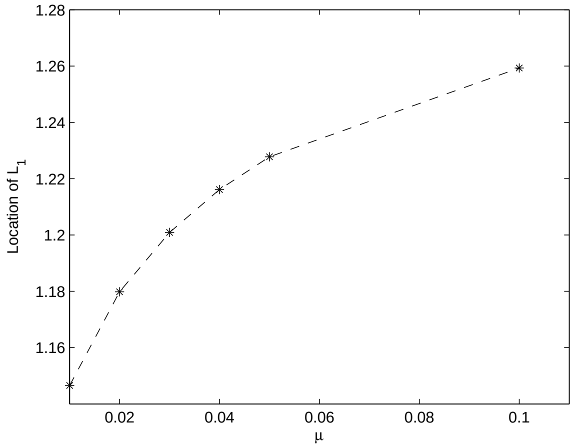

5(d): Classical with Relativistic

Figure 5: Position of L_1 with varying mass ratio of Saturn-Thethy.

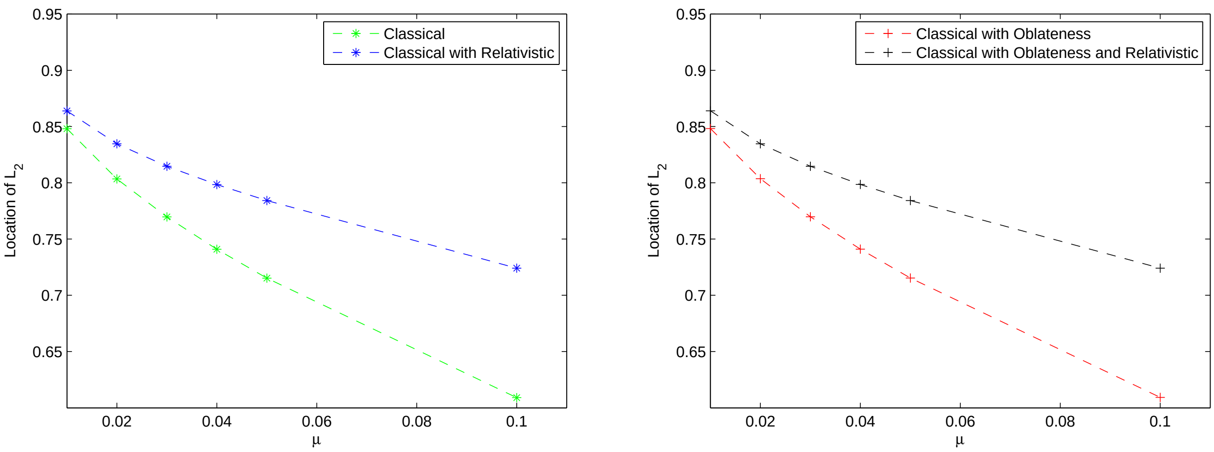

Figure 6: Position of L_2 with varying mass ratio of Jupiter-IO.

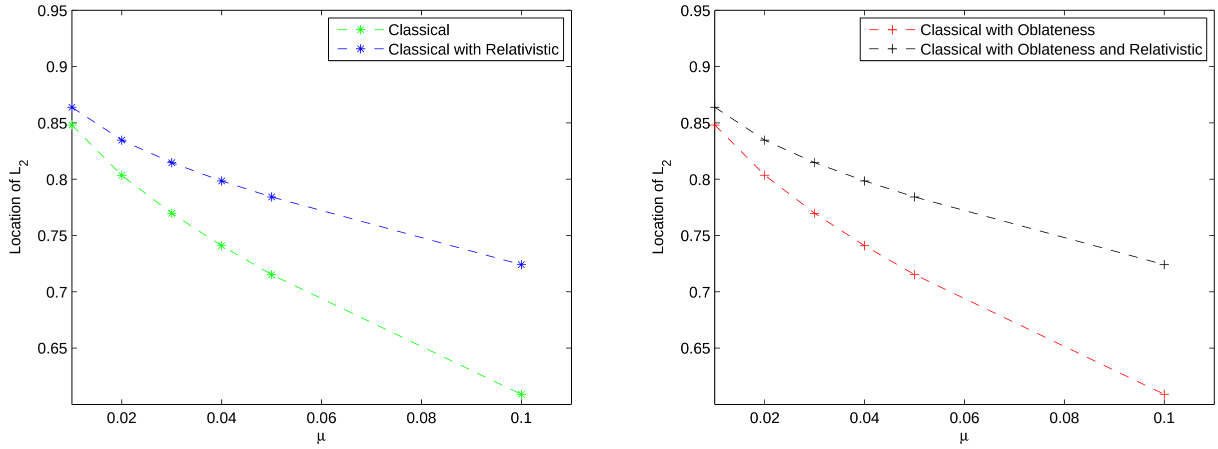

Figure 7: Position of L_2 with varying mass ratio of Jupiter-Europa.

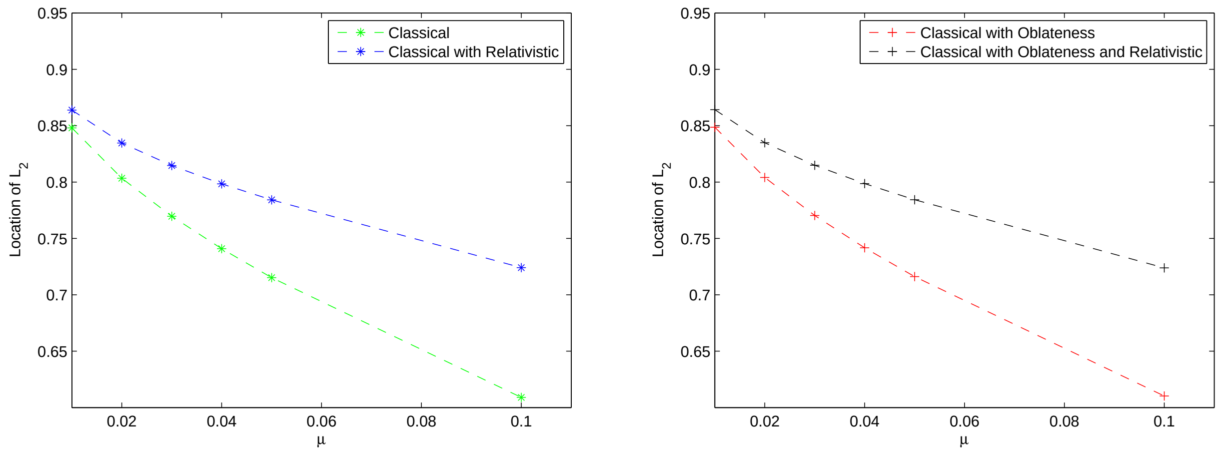

Figure 8: Position of L_2 with varying mass ratio of Saturn-Mimas.

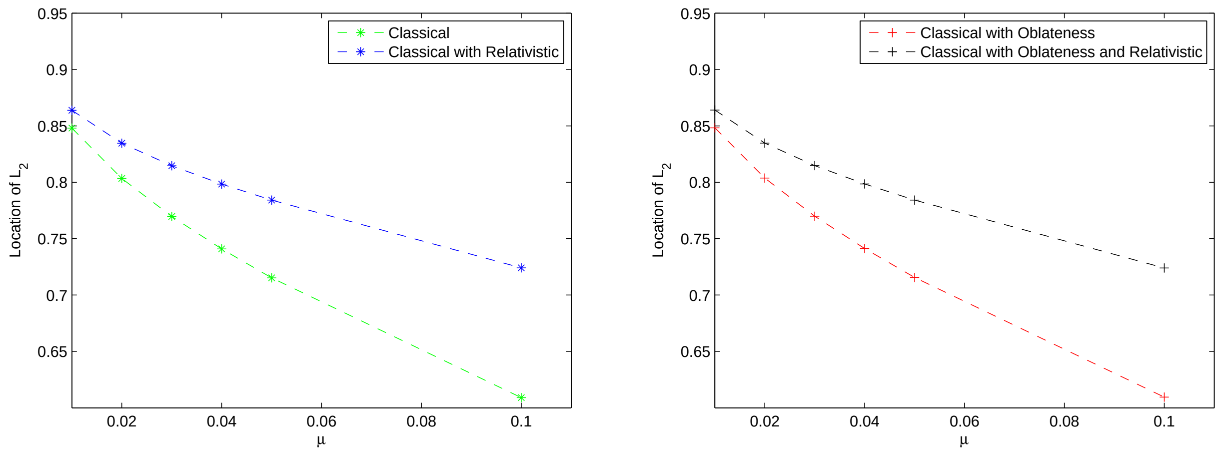

Figure 9: Position of L_2 with varying mass ratio of Saturn-Thethy.

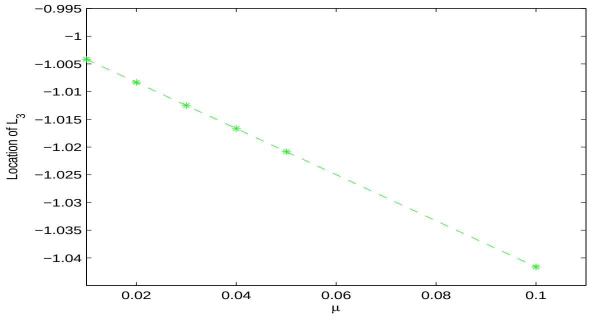

10(a): Classical

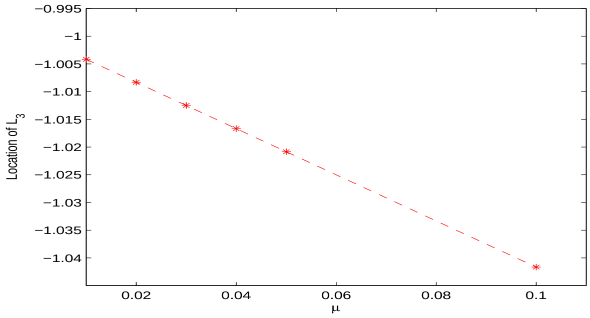

10(b): Classical with Relativistic

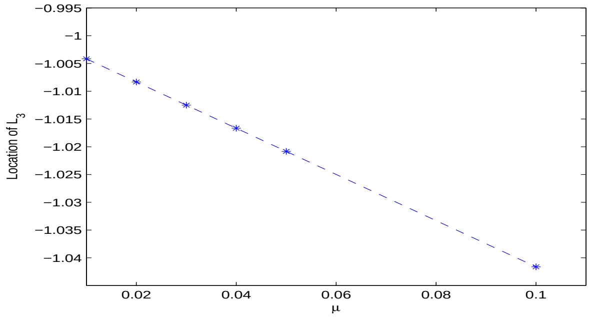

10(c): Classical

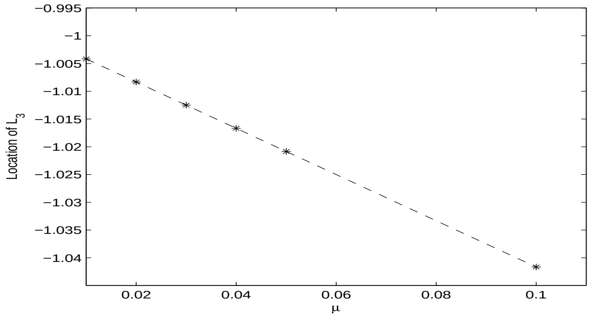

10(d): Classical with Relativistic

Figure 10: Position of L_3 with varying mass ratio of Jupiter-IO.

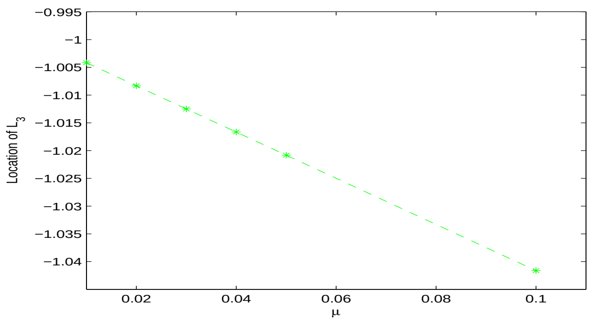

11(a): Classical

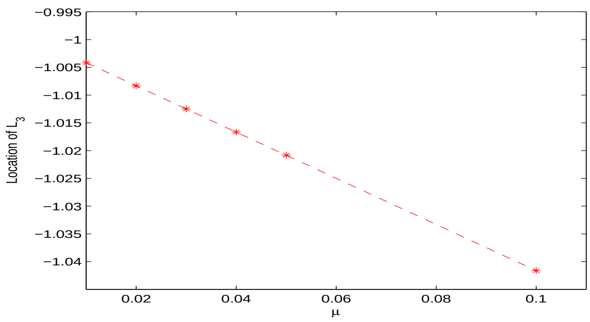

11(b): Classical with Relativistic

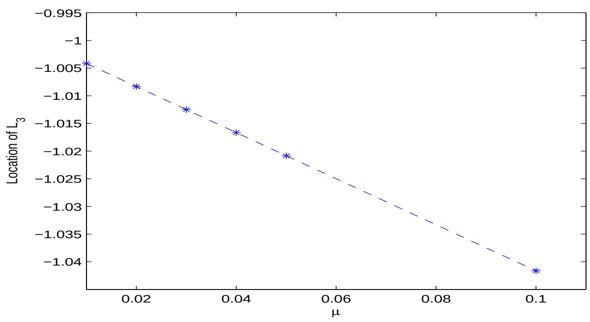

11(c): Classical

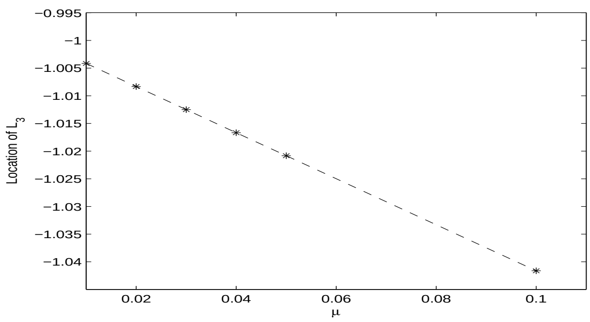

11(d): Classical with Relativistic

Figure 11: Position of L_3 with varying mass ratio of Jupiter-Europa.

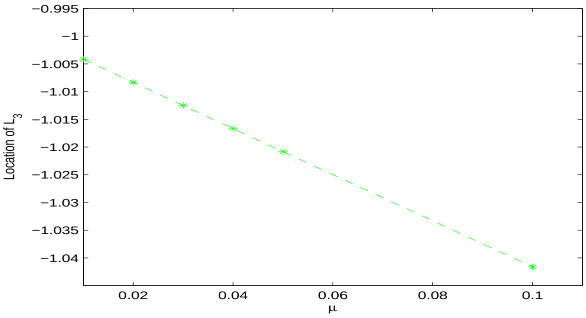

12(a): Classical

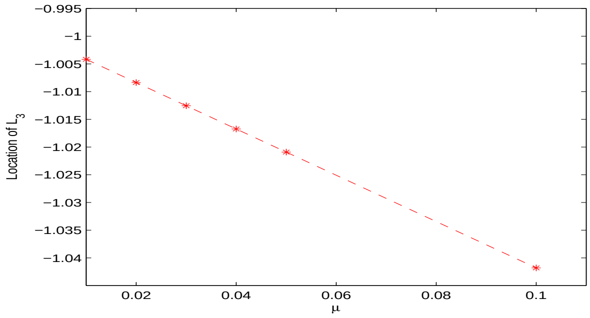

12(b): Classical with Relativistic

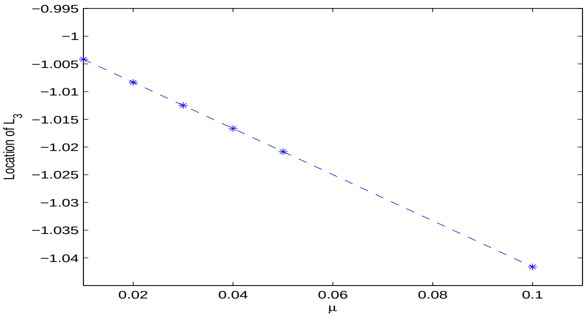

12(c): Classical

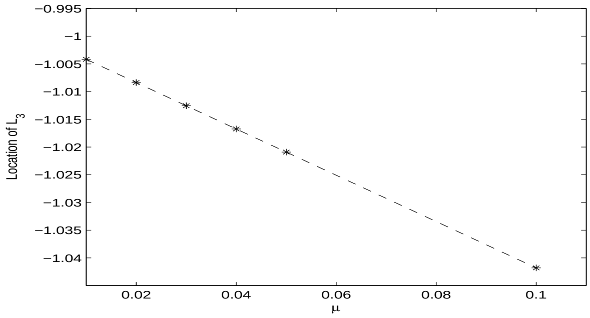

12(d): Classical with Relativistic

Figure 12: Position of L_3 with varying mass ratio of Saturn-Mimas.

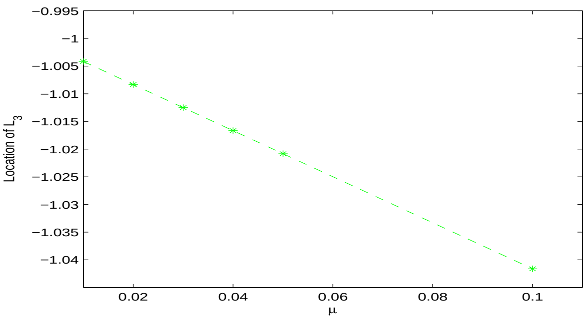

13(a): Classical

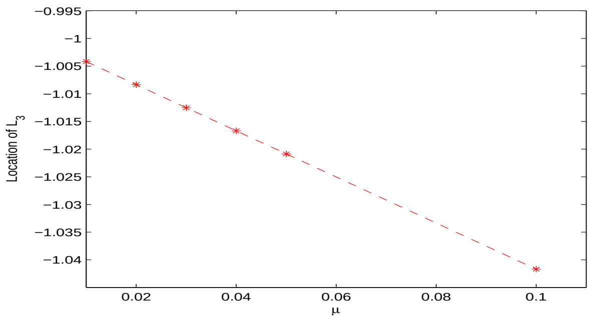

13(b): Classical with Relativistic

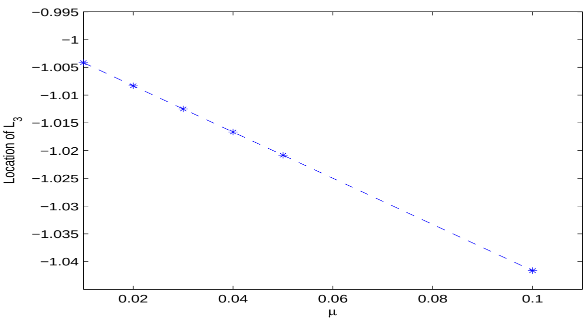

13(c): Classical

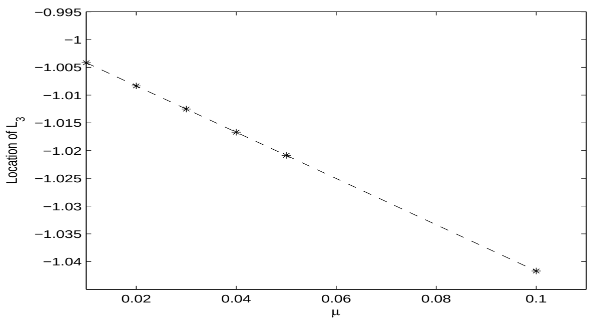

13(d): Classical with Relativistic

Figure 13: Position of L_3 with varying mass ratio of Saturn-Thethy.

are similar and may overlap if there are plotted on the same coordinate system. This indicates that the oblateness and relativistic factor does not have significant effects on L_1 when varying mass ratio μ (see Figs. 2-5); L_2 is moving towards the bigger primary as μ increase for each system. It is also interesting to observe from Figs. 6-9 that the graph of the position of L_2 in the presence of relativistic is always on the above of the graph of position of L_2 without relativistic for each case. This indicates that the relativistic terms have a significant effect on the position of L_2 when varying the mass ratio. Also, by inspection of the graphs of classical and classical with oblateness for each system it appears that, the two graphs are similar and if they are on the same coordinate system they may overlap. This indicates that the oblateness effect is not significant when varying mass ratio on the position of L_2; it is also observed that L_3 is moving away from the bigger primary as mass ratio μ increases for each system. Similarly it is seen from each figure of each system that the four graphs may overlap if they are plotted on the same coordinate system. This indicates that the oblateness and relativistic factors do not have significant effect on the position of L_3 when varying mass ratio (see Figs. 10-13).

The stability of collinear points of the considered binary systems have been investigated by finding the roots of the characteristic Eq.(13) as shown in Tables 3-5. It was observed that there exists at least a positive real root or positive real part of roots among all and hence the collinear points are unstable.

7 Conclusions

In the present paper we have obtained the locations of the collinear equilibrium points and studied their linear stability numerically in the neighbourhood of Jupiter-Satellite and Saturn-Satellite systems. The effect of oblateness is seen to cause a shift of L_1 and L_2 towards the smaller primary and L_3 to move away from the bigger primary for each system. As well, the relativistic factor causes a shift of L_1 and L_2 towards the smaller primary and has no significant effect on L_3 for each system. With an increase of the mass ratio we observed that, L_1 is moving away from the smaller primary, while L_2 is moving towards the bigger primary but L_3 is moving away from the bigger primary. Also, there is a noticeable impact of relativistic factor on L_2 when the mass ratio is increasing.

Acknowledgments

The authors are grateful to Prof. J. Singh for his valuable suggestions.

References

[1] P.V. SubbaRao and R.K. Sharma. A note on the stability of triangular points of equilibrium in the restricted three-body problem when the primaries are oblate spheroids. *Astron & Astrophys.*, 43(1975): 381–387.

[2] R.K. Sharma and P. V. SubbaRao. Collinear equilibria and their characteristic exponents in the restricted three-body problem when the primaries are oblate spheroids. *Celest. Mech.*, 12(1975): 189–201.

[3] R.K. Sharma. The linear stability of libration points of the photogravitational restricted three-body problem when the smaller primary is an oblate spheroid. *Astrophys Space Sci.*, 135(1987): 271–281.

[4] E.I. Abouelmagd. Existence and stability of triangular points in the restricted three-body problem with numerical applications. *Astrophys Space Sci.*, 342(2012): 45–53.

[5] R.L. Anderson, S. Campagnola and G. Lantoine. Broad search for unstable resonant orbits in the planar circular restricted three-body problem. *Celest. Mech. Dyn. Astr.*, 124(2016): 177–199.

[6] S.V. Ershkov. The Yarkovsky effect in generalized photogravitational 3-body problem. *Planetary Ershkov and Space Science.*, 73(2012): 221–223.

[7] A. Brumberg. Relativistic Celestial Mechanics. Nauka, Moscow. 1972.

[8] K.B. Bhatnagar and P.P. Hallan. Existence and stability of $L_{4,5}$ in the relativistic restricted three-body problem. *Celest. Mech. Dyn. Astr.*, 69(1998): 271–281.

[9] V. Szebehely. Theory of orbits: The restricted problem of three-bodies. Academic Press. New York. 1967.

[10] C.N. Douskos and E.A. Perdios. On the stability of equilibrium points in the relativistic restricted three-body problem. *Celest. Mech. Dyn. Astr.*, 82(2002): 317–221.

[11] M.K. Ahmed, F.A. Abd El-Salam and S.E. Abd El- Bar. On the stability of triangular Lagrangian equilibrium points in the relativistic restricted three-body problem. *American Journal of Applied Sciences.*, 3(2006): 1993–1998.

[12] J. Singh and N. Bello. Motion around L_4 in the perturbed relativistic R3BP. *Astrophys. Space Sci.*, 351(2014): 491–497.

[13] J. Singh and N. Bello. Effect of radiation pressure on the stability of $L_{4,5}$ in the relativistic restricted three-body problem. *Astrophys. Space Sci.*, 351(2014): 483–490.

[14] O. Ragos, E.A. Perdios, V.S. Kalantonis and M.N. Vrahatis. On the equilibrium points of the relativistic restricted three-body problem. *Nonlinear Analysis.*, 47(2001): 3413–3418.

[15] S.E. Abd El-Bar and F.A. Abd El-Salam. Computation of the locations of the libration points in the relativistic restricted three-body problem. *American Journal of Applied sciences.*, 9(2012): 659–665.

[16] S.E. Abd El-Bar and F.A. Abd El-Salam. Analytical and semi analytical treatment of the collinear points in the photogravitational relativistic R3BP. *Math. Problems Eng. Article 794734.*, (2013). http://dx.doi.org/10.1155/2013/794734

[17] F.A. Abd El-Salam and S.E. Abd El-Bar. On the triangular equilibrium points in the photogravitational relativistic restricted three-body problem. *Astrophys. Space Sci.*, 349(2014): 125.

[18] D.A. Katour, F.A. Abd El-Salam and M.O. Shaker. Relativistic restricted three-body problem with oblateness and photo-gravitational corrections to triangular equilibrium points. *Astrophys Space Sci.*, 351(2014): 143–149.

[19] N. Pushparaj and R.K. Sharma. Oblateness effect of Saturn on Halo orbits of $L_1\, and\, L_2$in Saturn-satellites Restricted Three-Body Problem. *I. J. A. A.*, 6(2016): 347–377.

[20] S.E. Abd El-Bar, F.A. Abd El-Salam and M. Rassem. Perturbed location of L_1 point in the photogravitational relativistic R3BP with oblate primaries. *Can. J. Phys.*, 93(2015): 300–311.

[21] F.A. Abd El-Salam, D.A. Katour and M.O. Shaker. On the equilibrium point L_1 in the photogravitational oblate relativistic R3BP with application on Sun-planate systems. *Eur. Phys. J. Plus.*, 130(2015).

[22] N. Bello and A.A. Hussain. Collinear equilibrium points in the relativistic R3BP when the bigger primary is a triaxial rigid body. *International Frontier Science Letters.*, 11(2016): 45–56.

[23] S.W. McCuskey. Introduction to celestial mechanics. Addision-Wesley. 1963.

[24] C.D. Murray and S.F. Dermott Solar System Dynamics. Cambridge University Press. 1999.